

A Preorganized Siderophore: Thermodynamic and Structural Characterization of Alcaligin and Bisucaberin, Microbial Macrocyclic Dihydroxamate Chelating Agents¹

Zhiguo Hou, Kenneth N. Raymond,* Brendon O'Sullivan, and Todd W. Esker

Department of Chemistry, University of California at Berkeley, Berkeley, California 94720

Takayuki Nishio

Osaka City Institute of Public Health and Environmental Science, 8-34 Tojo, Osaka, Japan

Received August 25, 1998

The iron coordination chemistry of two macrocyclic dihydroxamate siderophores, alcaligin (AG) and bisucaberin (BR), has been investigated thermodynamically and structurally. Alcaligin is a siderophore of freshwater bacteria as well as mammalian pathogens, including the bacterium that causes whooping cough in humans, while bisucaberin, a structural analogue of alcaligin, is produced by marine bacteria. Both alcaligin and bisucaberin form 1:1 ferric complexes (FeL^+) in acidic conditions and 2:3 ferric complexes (Fe_2L_3) at and above neutral pH. The stability constants of these macrocyclic dihydroxamate siderophores differ significantly from that of rhodotorulic acid (RA), a linear dihydroxamate siderophore. Notably, K_{FeL} of alcaligin is 32 times greater than that of rhodotorulic acid, while the subsequent stepwise formation constant for Fe_2L_3 is 3 times less. The Fe(III) complexes of alcaligin are stereospecific; the absolute configuration of the Fe_2L_3 complex (circular dichroism and X-ray structure) is Λ . The structure of the Fe_2L_3 alcaligin complex is a topological alternative to the triple-helicate structure of the rhodotorulic complex $\text{Fe}_2(\text{RA})_3$. The structures of the free ligand and the bisbidentate ligand in the FeL complex are essentially identical, indicating that alcaligin is highly preorganized for metal ion binding. This explains the difference in K_{FeL} between alcaligin and rhodotorulic acid, as well as explaining the monobridged topology of the Fe_2L_3 alcaligin complex. The protonation constants ($\log K_{a1}$ and $\log K_{a2}$) are 9.42(5) and 8.61(1) for alcaligin and 9.49(2) and 8.76(3) for bisucaberin. The stepwise formation constants of the Fe(III) complexes ($\log K_{\text{ML}}$ and $\log K_{\text{M}_2\text{L}_3}$) are 23.5(2) and 17.7(2) for alcaligin and 23.5(5) and 17.2(5) for bisucaberin. The overall formation constants ($\log \beta_{230}$) of alcaligin and bisucaberin are 64.7(1) and 64.3(1). The solution chemistry of Fe(III) and alcaligin was further investigated at a lower ligand to metal ratio (1:1). At high pH, a novel 2:2 ferric bis- μ -oxo-bridged complex of alcaligin forms ($\text{Fe}_2\text{L}_2\text{O}_2^{2-}$) with a $\log \beta_{22-4}$ of 16.7(2). This species exhibits behavior consistent with an iron bis- μ -oxo complex, including antiferromagnetic coupling. Crystal data: $\text{Fe}_2(\text{AG})_3 \cdot 25\text{H}_2\text{O}$ crystallizes in the orthorhombic space group $P2_12_12_1$ with $a = 13.3374(4)$ Å, $b = 16.1879(5)$ Å, $c = 37.886(1)$ Å, $V = 8179.7(4)$, $Z = 4$. For 5512 reflections with $F_o^2 > 3\sigma(F_o^2)$ the final R (R_w) = 0.053(0.068).

Introduction

Most aerobic and anaerobic bacteria and fungi synthesize and excrete low molecular weight compounds, siderophores, for the solubilization and transport of iron.^{2–5} Siderophores form strong and selective complexes with Fe(III) which are usually taken up via membrane receptors. The recognition and transport of these complexes is generally stereoselective, primarily recognizing the metal ion coordination geometry.^{4,6} Since iron is required by all except a few microorganisms, and certainly by all pathogenic bacteria, understanding siderophore-mediated iron

transport is a significant problem in both bioinorganic chemistry and medicine.

Alcaligin is a 20-membered macrocyclic dihydroxamate siderophore (Figure 1). It was first isolated from an aquatic algae, *Alcaligenes xylosoxidans* subsp. *xylosoxidans*,⁷ and recently from two pathogenic bacteria, *Bordetella pertussis* and *Bordetella bronchiseptica*.^{8,9} Although the bacterium *A. xylosoxidans* is normally noninfectious, it has occasionally been observed to cause disease in immunocompromised patients.^{10,11}

* Author to whom correspondence should be addressed.

- (1) Coordination Chemistry of Microbial Iron Transport. 65. Part 64; Telford, J. R.; Raymond, K. N. *Inorg. Chem.* **1998**, *37*, 4578–4583.
- (2) Neilands, J. B. *Biophys.* **1993**, *302*, 1–3.
- (3) Telford, J. R.; Raymond, K. N. In *Comprehensive Supramolecular Chemistry*; Atwood, J. L., Davies, J. E. D., MacNicol, D. D., and Vogtle, F., Eds.; Elsevier Science Ltd.: Oxford, 1996; Vol. 1, pp 245–266.
- (4) Matzanke, B. F.; Müller-Matzanke, G.; Raymond, K. N. In *Iron Carriers and Iron Proteins*; Loehr, T. M., Ed.; Physical Bioinorganic Chemistry Series; VCH Publishers: New York, 1989 pp 1–121.
- (5) Wooldridge, K. G.; Williams, P. H. *FEMS Microbiol. Rev.* **1993**, *12*, 325–348.

- (6) van der Helm, D.; Jalal, M. A. F.; Hossain, M. B. In *Iron transport in microbes, plants, and animals*; VCH Publishers: New York, 1987; pp 135–139.
- (7) Nishio, T.; Tanaka, N.; Hiratake, J.; Katsube, Y.; Ishida, Y.; Oda, J. *J. Am. Chem. Soc.* **1988**, *110*, 8733–8734. The organism's name has been changed: Kiredjian, M.; Holmes, B.; Kersters, K.; Guilvout I.; Deley, J. *Int. J. Syst. Bacteriol.* **1986**, *36*, 282–287.
- (8) Moore, C. H.; Foster, L.-A.; Gerbig, D. G., Jr.; Dyer, D. W.; Gibson, B. W. *J. Bacteriol.* **1995**, *177*, 1116–1118.
- (9) Brickman, T. J.; Hansel, J.-G.; Miller, M. J.; Armstrong, S. K. *Biomaterials* **1996**, *9*, 191–203.
- (10) Decre, D.; Arlet, G.; Danglot, C.; Lucet, J. C.; Fournier, G.; Bergogne-Berezin, E.; Philippon, A. *J. Antimicrob. Chemother.* **1992**, *30*, 769–779.
- (11) Hearn, Y. R.; Gander, R. M. *Am. J. Clin. Pathol.* **1991**, *96*, 211–214.

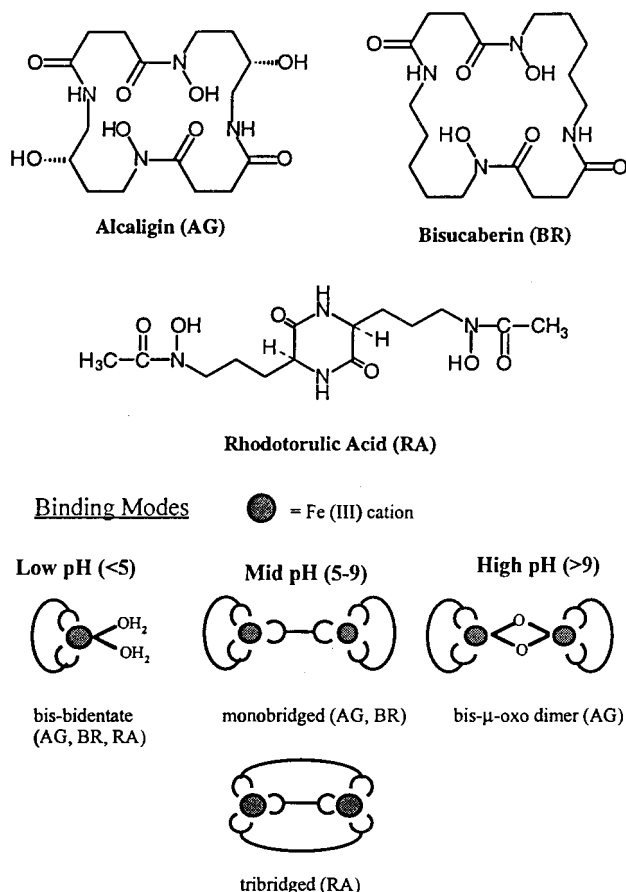


Figure 1. Siderophore ligand structures and binding modes discussed in this paper.

In contrast, *B. pertussis* and *B. bronchiseptica* are obligate pathogens of the upper respiratory tract of their mammalian hosts. The former causes human whooping cough,¹² while the latter is the agent of swine atrophic rhinitis and kennel cough in dogs.¹³ As mucosal pathogens, these bacteria adhere and multiply in a niche bathed in iron-sequestering host glycoproteins.

Structurally similar to alcaligin (Figure 1), bisucaberin is a 22-membered macrocyclic dihydroxamate siderophore isolated from the marine bacterium *Alteromonas hyloplanktis*.¹⁴ It was found to slow the growth of both L-1210 and 1MC carcinoma cell with IC₅₀s of 9.7 and 12.7 μ M, respectively, and to sensitize tumor cells to macrophage-promoted cytolysis.¹⁵ This ability was proposed to arise from the trapping of iron within the cell, thereby preventing the metal from participating in mitochondrial respiration.

In addition to their biological and medical significance, alcaligin and bisucaberin are also of interest with respect to their coordination chemistry. Among more than 200 siderophores isolated to date, alcaligin and bisucaberin represent a new structural class of siderophores, endocyclic dihydroxamates. The coordination chemistry of this class is essentially unknown.¹⁶

The tetradentate nature of these ligands is particularly interesting, since they are unable to satisfy the preferred

octahedral coordination geometry of Fe(III) by forming a simple 1:1 complex. In order to encapsulate completely the metal ion, a dihydroxamate siderophore must form minimally a binuclear metal complex with a stoichiometry of Fe₂L₃ (L represents a dihydroxamate dianion). An early example is provided by rhodotorulic acid (Figure 1), a linear dihydroxamate siderophore of *Rhodotorula mucilaginosa* (previously *R. pilimanae*), which forms a complex of stoichiometry Fe₂L₃,^{17,18} as does a synthetic hydroxypyridonate analogue.¹⁹ Today these complexes are classed as triple helicates in the nomenclature of supramolecular chemistry.²⁰

As shown in Figure 1, the Fe₂L₃ stoichiometry can be equally satisfied by two different topologies, the monobridged dimer and the triple helicate. A preliminary report described the characterization of the monobridged structure.²¹ Presented here is an investigation of these macrocyclic dihydroxamate siderophores, including solution thermodynamic characterization of alcaligin and bisucaberin and the crystal structure of the Fe₂L₃ complex of alcaligin. Remarkably, alcaligin and bisucaberin are highly preorganized for metal ion chelation. This stereochemical feature of these cyclic siderophores not only enforces a monobridged molecular assembly but also distinguishes its solution thermodynamic properties from a linear dihydroxamate siderophore, such as rhodotorulic acid.

Results and Discussion

Solution Thermodynamics Studies. Free Ligands. Ligand protonation constants were determined by potentiometric titration. Alcaligin is a weak diprotic acid. Proton exchange is associated with the ligands' two hydroxamate groups. The ligand is very soluble in water and gives a colorless solution. Three samples were titrated to increasing and decreasing pH within the range 3–11. Two protonation constants were determined to be log K_{a1} = 9.42(5) and log K_{a2} = 8.61(1).

It was reported that bisucaberin is nearly insoluble in water.²² However, in our experiments no precipitate was observed with ligand concentrations near 0.5 mM, although dissolution in water was slow. Due to a limited supply of the ligand, only one sample was titrated, from pH 11 to pH 3 and back to pH 11. The protonation constants of bisucaberin, log K_{a1} = 9.49(2) and log K_{a2} = 8.76(3), are very close to those of alcaligin, as expected.

Spectral Signatures: Ferric Complexes. The vis/UV spectra of these dihydroxamate siderophores closely resemble the values observed for rhodotorulic acid (RA).¹⁷ Metal:ligand stoichiometries were kept at 2:3.5. At pH 2.5, alcaligin (AG) and bisucaberin (BR) gave λ_{max} = 472 nm (ϵ = 2.0 \times 10³ cm⁻¹ M⁻¹/Fe), which confirms the dihydroxamate coordination environment around the iron and corresponds to the red FeL⁺ complex. From pH 6–9, both siderophore complexes gave absorbances at λ_{max} = 428 nm (ϵ = 2.7 \times 10³ cm⁻¹ M⁻¹/Fe) and λ_{max} = 426 nm (ϵ = 2.7 \times 10³ cm⁻¹ M⁻¹/Fe), respectively,

(12) Wardlaw, A. C.; Parton, R. In *Pathogenesis and Immunity in Pertussis*; John Wiley & Sons: New York, 1988; pp 327–352.

(13) Goodnow, R. A. *Microbiol. Rev.* **1980**, *44*, 722–738.

(14) Takahashi, A.; Nakamura, H.; Kameyama, T.; Kurasawa, S.; Nagawana, H.; Okami, Y.; Takeuchi, T.; Umezawa, H. *J. Antibiot.* **1987**, *110*, 1671–1676.

(15) Kameyama, T.; Takahashi, A.; Kurasawa, S.; Ishizuka, M.; Okami, Y.; Takeuchi, T.; Umezawa, H. *J. Antibiot.* **1987**, *110*, 1664–1670.

(16) Konetschny-Rapp, S.; Jung, G.; Raymond, K. N.; Meiwes, J.; Zahner, H. *J. Am. Chem. Soc.* **1992**, *114*, 2224–2230. Another cyclic siderophore has been reported: Ledyard, K. M.; Butler, A. *J. Biol. Chem.* **1997**, *2*, 93–97.

(17) Carrano, C. J.; Raymond, K. N. *J. Am. Chem. Soc.* **1978**, *100*, 5371–5374.

(18) Carrano, C. J.; Cooper, S. R.; Raymond, K. N. *J. Am. Chem. Soc.* **1979**, *101*, 599–604.

(19) Scarrow, R. C.; White, D. L.; Raymond, K. N. *J. Am. Chem. Soc.* **1985**, *107*, 6540–6546.

(20) Caulder, D. L.; Raymond, K. N. *Angew. Chem.* **1997**, *36*, 1439–1442.

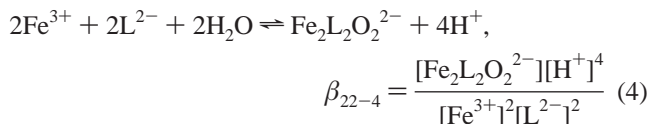
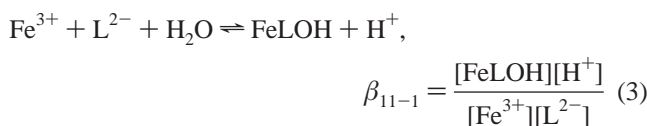
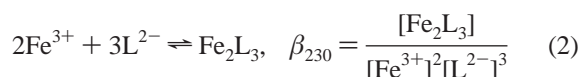
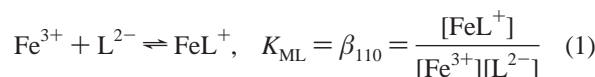
(21) Hou, Z.; Sunderland, C. J.; Nishio, T.; Raymond, K. N. *J. Am. Chem. Soc.* **1996**, *118*, 5148–5149.

(22) Bergeron, R. J.; McManis, J. S. *Tetrahedron* **1989**, *45*, 4939–4944.

which is typical of the ligand to metal charge transfer transition of a trihydroxamate ferric complex⁴ and corresponds to the orange species, Fe₂L₃. At pH 11, the ferric alcaligin complex produces a yellow solution with λ_{max} = 382 nm (ε = 1.7 × 10³ cm⁻¹ M⁻¹/Fe), which is characteristic of Fe bis-μ-oxo dimers.²³

Solution Thermodynamics: Ferric Complexes. The stepwise and overall stability constant equations for the iron complexes are defined below (eqs 1–9). Some charges are omitted in eq 11 for clarity. Note that the activity of water, H₂O, has been set to 1. The values for both alcaligin and bisucaberin are described below and summarized in Table 1.

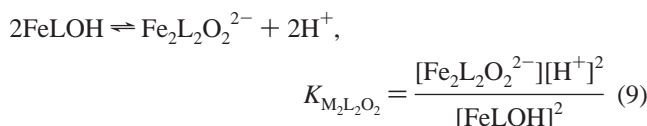
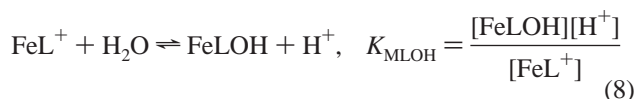
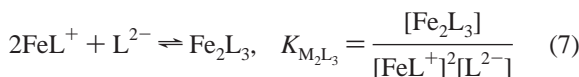
overall stability constant equations



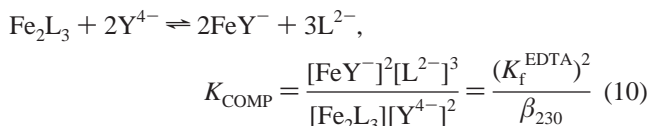
$$\beta_{230} = (K_{\text{ML}})^2 K_{\text{M}_2\text{L}_3} \quad (5)$$

$$\beta_{22-4} = (\beta_{11-1})^2 K_{\text{M}_2\text{L}_2\text{O}_2} \quad (6)$$

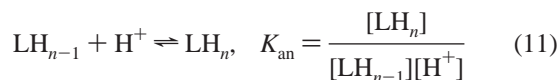
stepwise stability constant equations



competition titration equation



protonation constant equation



Alcaligin. The overall stability constants (β values) for the ferric complexes are described by eqs 1–4. Indirect methods were employed to probe the equilibria because the ligand is always bound to Fe(III) from pH 2 to 11. The constant β₂₃₀ was determined by competition titrations with EDTA using the

Table 1. Thermodynamic Parameters for Alcaligin, Bisucaberin, and Rhodotorulic Acid^a

	AG	BR	RA ^b
Protonation constants			
log K _{a1}	9.42(5)	9.49(2)	9.44(3)
log K _{a2}	8.61(1)	8.76(3)	8.49(3)
Determined Formation Constants with Fe ³⁺			
log β ₁₁₀ = log K _{ML}	23.5(2)	23.5(2)	21.99(6)
log β ₂₃₀	64.7(1)	64.3(1)	62.2(1)
log β ₁₁₋₁	17.2(1)		
log β ₂₂₋₄	16.7(2)		
Derived Stepwise Formation Constants			
log K _{M₂L₃}	17.7	17.2	18.22
log K _{MLOH}	-6.3		
log K _{M₂L₂O₂}	-17.7		
pM ^c	23.0	22.5	21.9

^a Errors are given in parentheses after each figure as an integer value for the least significant digit. These are the standard deviations derived from the nonlinear least squares refinements. ^b From ref 18, ionic strength 0.1 M. In our preliminary report (ref 21) stability constants for 0.1 and 1.0 M ionic strength were (incorrectly) compared. ^c pM = -log [Fe³⁺] at pH 7.4 with total ligand concentration = 10⁻⁵ M and total iron concentration = 10⁻⁶ M.

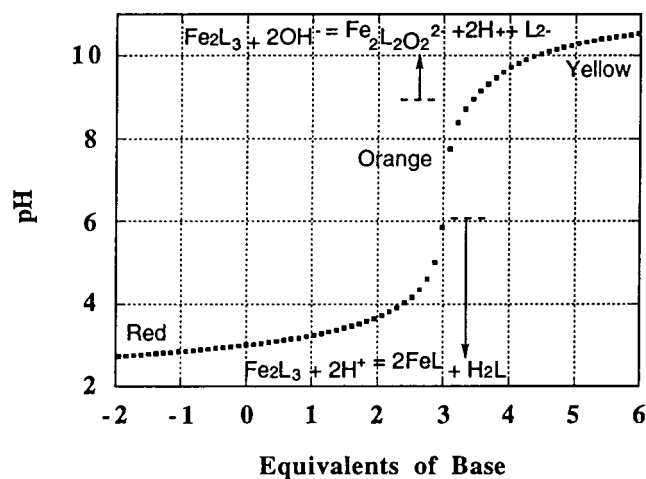


Figure 2. Potentiometric titration curve for 2:3.5 solution of ferric and alcaligin. The titration was carried out at 25 °C, μ = 0.100 M (KCl) with a ligand concentration 0.0950 mM.

known value of this stability constant.²⁴ In all, 25 samples from pH 6.0 to 8.3 were prepared with 10:1 EDTA:AG and 2:3.5 Fe:AG ratios. Attainment of equilibrium was determined by following the visible spectra (Figure 3). Log β₂₃₀ was then calculated (from eq 10) as 64.7(1).

As the pH decreases from 5 to 2, the orange solution of the Fe₂L₃ alcaligin complex turns red, indicating a change in the iron coordination environment from tri- to bihydroxamate. Three sets of potentiometric data in this pH range were fit for eq 7. Spectrophotometric data (Figure 3) showed an isosbestic point at 478 nm and confirmed the potentiometric results. As the pH increases from 9 to 11, the orange solution of the Fe₂L₃ alcaligin complex turns yellow (Figure 3), indicating the formation of a third complex at high pH. Potentiometric titrations were undertaken for 1:1 Fe:AG solutions to augment the spectrophotometric titration data.

Under these conditions there is insufficient ligand present for formation of the Fe₂L₃ species. Instead the FeL⁺ species hydrolyzes to give the ternary complex FeLOH according to

(23) Kurtz, D. M., Jr. *Chem. Rev.* **1990**, *90*, 585–606.

(24) Martell, A. E.; Smith, R. M. *Critical Stability Constants*; Plenum: New York, 1976; Vol. IV.

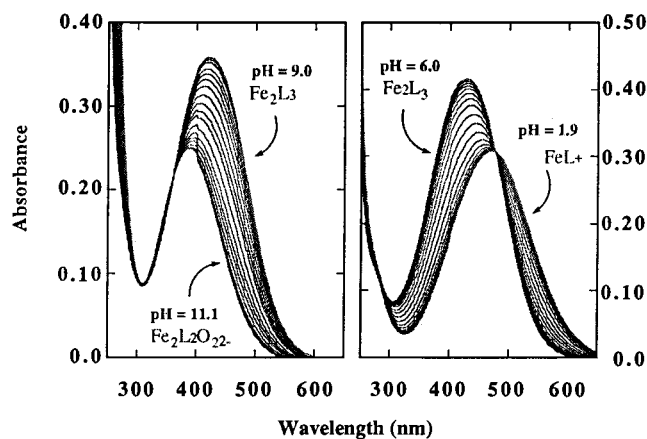


Figure 3. Vis/UV spectra of a 2:3.5 solution of ferric ion and alcaligin as a function of pH, [alcaligin] = 0.026 68 mM, $\mu = 0.100$ M (KCl), $T = 25$ °C.

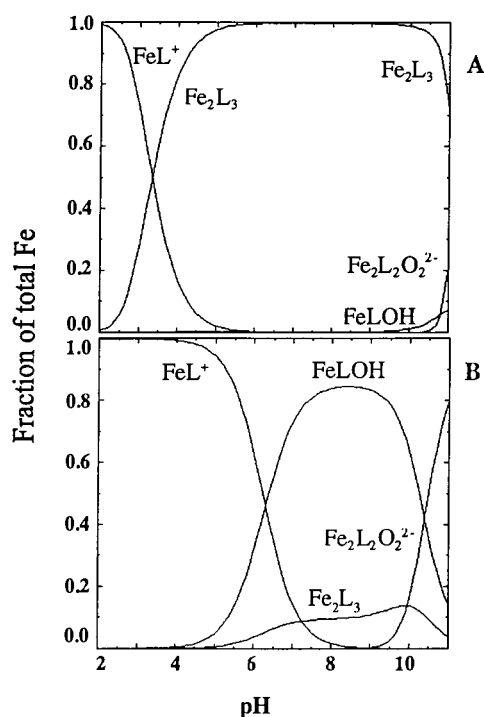


Figure 4. Species distribution diagrams for the system $H^+/Fe^{3+}/$ alcaligin. Total metal and ligand concentrations are (A) $[Fe] = 1$ mM, [alcaligin] = 1.75 mM (Fe:AG = 2:3.5) and (B) $[Fe] = 1$ mM, [alcaligin] = 1 mM (Fe:AG = 1:1).

eq 8. In this reaction the complex behaves as a weak acid with a pK_a value of 6.3 ($\log K_{MLOH} = -6.3$, Table 1).

At higher pH the hydroxy complex dimerizes to the bis- μ -oxo species $Fe_2L_2O_2^{2-}$. A close fit was achieved in refinement of the potentiometric data with a $\log \beta_{22-4}$ value of 16.7(2). The pH of the midpoint of this transition, i.e. where $[FeLOH] = [Fe_2L_2O_2^{2-}]$, will have a dependence on the absolute concentration of the species $[FeLOH]$. This is because the term for $[FeLOH]$ is squared in the expression for $K_{M_2L_2O_2}$ in eq 9. For the conditions employed here (1:1 Fe:AG) this transition occurs at pH 10.4.

Figure 4 gives species distribution diagrams for Fe(III) and alcaligin. Two limiting cases are illustrated which give complete (or near complete) formation of each of the complexes and correspond to the conditions used in the potentiometric titrations.

Bisucaberin. $\log \beta_{230}$ was determined in the same way as for alcaligin (competition with EDTA, eq 10). Eighteen samples

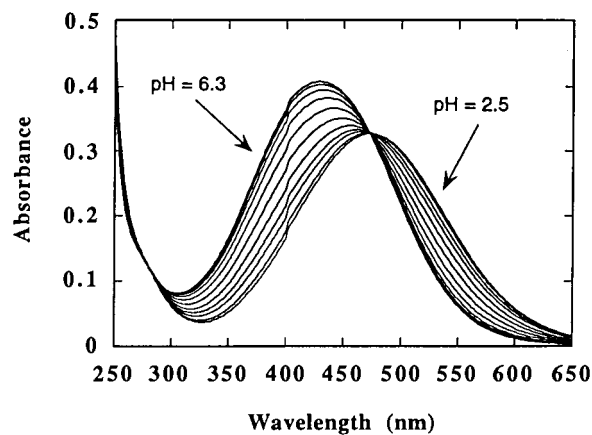


Figure 5. Vis/UV spectra of a 2:3.6 solution of ferric ion and bisucaberin as a function of pH, [bisucaberin] = 0.0243 mM, $\mu = 0.100$ M (KCl), $T = 25$ °C.

Table 2. Stability Constants and pM Values of the Ferric Complexes of Some Hydroxamate Siderophores (from Refs 16 and 25) Compared with Alcaligin and Bisucaberin

ligands	$\log \beta$	pM ^a
ferrioxamine E	32.5	27.7
ferrioxamine B	30.5	26.6
ferrioxamine D ₁	30.76	
ferricrocin	30.4	26.5
ferrichrysin	30.3	25.8
ferrichrome A	32.0	
ferrichrome	29.1	25.2
coprogen	30.2	27.5
rhodotorulic acid	31.2 ^b	21.9
alcaligin	32.4 ^b	23.0
bisucaberin	32.2 ^b	22.5

^a pM = $-\log [Fe^{3+}]$ at pH 7.4 with total ligand concentration = 10^{-5} M and total iron concentration = 10^{-6} M. ^b $1/2 (\log \beta_{230})$.

from pH 5.9 to 8.5 were tested after waiting 5 days for equilibrium. The overall stability constant of ferric bisucaberin complex, $\log \beta_{230}$, was determined to be 64.3(1). Potentiometric and spectrophotometric titrations of the ferric bisucaberin complex show that it is very similar to alcaligin. Figure 5 shows a family of spectra recorded in the pH range 2.5–6.3 for a solution (Fe:L = 2:3.6) of the ferric bisucaberin complex. Refinement of both potentiometric and spectrophotometric titration data resulted in almost identical equilibrium constants for the transition between FeL^+ and Fe_2L_3 ($\log K_{M_2L_3}$, 17.2). These data also gave an identical $\log \beta_{110}$ (K_{ML}), 23.5(5), indicating that bisucaberin's properties, including its preorganization, are identical to those of alcaligin. The behavior of bisucaberin with Fe(III) at low ligand to metal ratios, i.e., 1:1 bisucaberin:Fe, was not investigated due to the limited supply of this ligand.

Comparison of Siderophores. Table 2 lists stability constants and pM values of representative hydroxamate siderophores^{16,25} with alcaligin and bisucaberin. Since β_{230} represents a formation constant of two ferric ion centers, effective stability constants of alcaligin and bisucaberin per metal center are listed as $1/2 \log \beta_{230}$ (32.4 and 32.2, respectively). These values are about 2 orders of magnitude higher than those of other neutral hydroxamate siderophore complexes. The only exception is ferrioxamine E, which has an endocyclic trihydroxamate structure.¹⁶ Ferrichrome A forms an anionic chelate with Fe(III). It has been noted that hydroxamate siderophores display

(25) Crumbliss, A. L. In *CRC Handbook of Microbial Iron Chelates*; CRC Press: New York, 1991; pp 177–233.

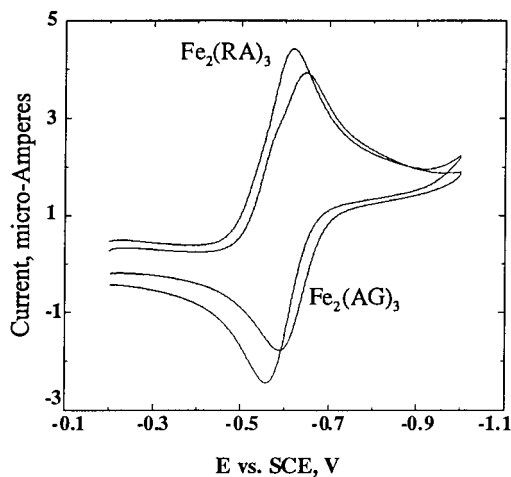


Figure 6. Cyclic voltammograms (scan rate = 100 mV/s) of $\text{Fe}_2(\text{RA})_3$ (pH 7.7) and $\text{Fe}_2(\text{AG})_3$ (pH 7.6).

no chelate effect beyond that of the bidentate hydroxamate groups;¹⁸ the stability constants of their ferric complexes generally depend only on the number of hydroxamates bound to Fe(III), not on whether they are separate or part of one molecule.

The substantial difference in stability constants between the first stepwise formation constant K_{ML} of alcaligin and rhodotorulic acid (Table 1) is remarkable and is directly attributable to the stereochemistry of the ferric alcaligin complex (*vide infra*).

Reduction Potential of the $\text{Fe}_2(\text{AG})_3$ Dimer. Hydroxamate siderophores appear generally to release iron through a one-electron reduction from the Fe(III) to the less stable Fe(II) complex.⁴ The reduction potential of AG at physiological pH is therefore another significant property for iron transport. Cyclic voltammetry showed that the AG ferric complex has a redox potential of -618 mV vs the standard calomel electrode (SCE) at pH 7.6 compared with the RA ferric complex at -588 mV at pH 7 (Figure 6).

Magnetic Susceptibilities of the Ferric Alcaligin Complexes. Solution magnetic data were recorded at pH 2, 7, and 11 for the different complexes. Rhodotorulic acid complexes were found to have μ_{eff} values consistent with no interaction between metal centers (6.0 for $\text{Fe}(\text{RA})^+$, 8.3 for $\text{Fe}_2(\text{RA})_3$).¹⁷ Comparable values were found for the analogous alcaligin complexes (5.8 for $\text{Fe}(\text{AG})^+$, 8.0 for $\text{Fe}_2(\text{AG})_3$). At high pH, however, a value of 5.4 is observed for the complex $\text{Fe}_2(\text{AG})_2\text{O}_2^{2-}$, which indicates antiferromagnetic coupling. This is typical for iron bis- μ -oxo dimers.

Circular Dichroism. The circular dichroism spectra of ferric alcaligin were studied in aqueous solution as a function of pH. As for the vis/UV spectra of ferric alcaligin, the CD spectra follow closely the species distribution calculated from the assigned thermodynamic values for ligand complexation and protonation. From pH 6 to 9, where the 2:3 species predominates, the CD spectrum is independent of pH (Figure 7). It consists of two CD peaks at 450 nm (+4.3) and 370 nm (-4.4) and a shoulder at 300 nm (-2.5). A decrease of pH causes a shift of CD peaks and reduction of intensity. The CD spectrum at pH 2.3, where the species FeL^+ predominates, displays three peaks at 320 nm (-1.5), 410 nm (1.8), and 495 nm (-2.1) consistent with predominantly Δ absolute configuration, as shown.

For the pseudooctahedral ferric complex (Fe_2L_3), the absolute configuration of the local D_3 symmetry complex can be assigned by comparing its CD spectrum to that of other trihydroxamate

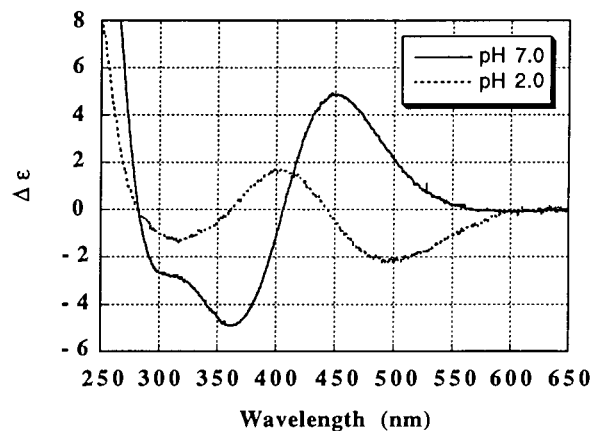


Figure 7. Circular dichroism spectra of a 2:3:4 solution of ferric ion and alcaligin recorded as a function of pH.

ferric complexes with known configuration, including the ferrichrome siderophores.⁴ The Fe_2L_3 complex of alcaligin has a positive Cotton effect at 450 nm, and its CD spectrum is qualitatively the same as those of the other trihydroxamate siderophores of Λ absolute configuration and is consistent with the Λ absolute configuration observed in the solid state (*vide infra*). This is opposite to the Δ chirality of the Fe_2RA_3 complex.¹⁷ The consequences to siderophore-mediated iron transport of the opposite chirality in the unnatural, mirror image siderophore, with corresponding opposite metal center chirality, have been explored in several siderophore systems,⁴ notably that of rhodotorulic acid and a ferrichrome uptake system.²⁶

The Structure of $\text{Fe}_2(\text{AG})_3$. An X-ray quality crystal of the 2:3 ferric complex of alcaligin, $\text{Fe}_2(\text{AG})_3$, was obtained from a solution of $\text{H}_2\text{O}/\text{CH}_3\text{CN}$. As illustrated in our previous communication,²¹ $\text{Fe}_2(\text{AG})_3$ adopts a monobridged topology with a U-shaped molecular conformation corresponding to the monobridged schematic in Figure 1. The bridging ligand twists significantly from the C_2 molecular symmetry. Each $\text{Fe}_2(\text{AG})_3$ molecule is surrounded by 25 water molecules, and each Fe^{3+} is coordinated in a pseudooctahedral environment provided by three hydroxamates. The absolute configuration is confirmed by the refinement and is consistent with the determination of the ligand structure by synthesis.²⁷ The metal centers, each being of Λ absolute configuration, are separated by 7.44 Å. The metrical parameters of the two symmetry-independent coordination centers (including twist angle, ligand bite and corresponding bond angle, and Fe–O distances) are essentially identical and are illustrated in the Supporting Information.

While most of the metrical parameters of $\text{Fe}_2(\text{AG})_3$ are very similar to those of other ferric hydroxamate complexes,⁶ including ferrichrome and ferrioxamine E, the geometric configuration and twist angles of $\text{Fe}_2(\text{AG})_3$ are distinctive. Among the 15 structurally characterized ferric hydroxamate complexes, the structure of $\text{Fe}_2(\text{AG})_3$ is only the second example of a trans coordination geometry for the relative orientations of the hydroxamate rings.⁶ This is a direct consequence of the ligand stereochemistry. When an alcaligin molecule binds a ferric ion, its two hydroxamate binding groups must be trans to each other, regardless of the metal center chirality generated. Since the free ligand has C_2 molecular symmetry, a cis coordination of the two hydroxamates is prohibited, due to the constraints of alcaligin's small cyclic ring.

(26) Müller, G.; Matzanke, B. F.; Raymond, K. N. *J. Bacteriol.* **1984**, *160*, 313–318.

(27) Bergeron, R. J.; McManis, J. S.; Perumal, P. T.; Algee, S. E. *J. Org. Chem.* **1991**, *56*, 5560–5563.

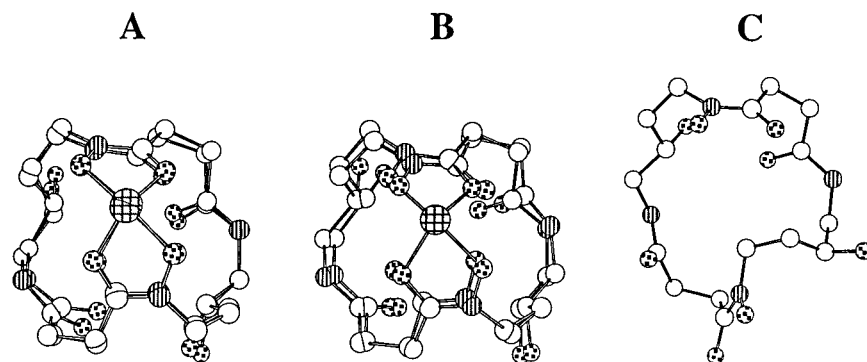


Figure 8. Overlays of structural fragments: (A) overlay of the two terminal fragments in the mono-bridged structure (as shown in Figure 1); (B) one of the terminal ligands from the complex over the free ligand structure; (C) the central, bridging fragment of $\text{Fe}_2(\text{AG})_3$. Iron atoms are indicated by cross hatching, vertical lines indicate nitrogen atoms, and oxygen atoms are filled with dots. The remaining atoms are carbon.

The small ligand ring size and resultant steric constraint imposed by the ligand are also reflected in the relatively smaller twist angles (33.0° and 33.1°) of the structure of $\text{Fe}_2(\text{AG})_3$. For the 14 previously characterized ferric hydroxamate structures, twist angles range from 41° to 45° ,⁶ about 10° greater than that of the $\text{Fe}_2(\text{AG})_3$ structure. The twist angles of the $\text{Fe}_2(\text{AG})_3$ structure are also significantly smaller than calculated from the Kepert model;²⁸ the theoretical twist angle is calculated as 44° for the complex with a normalized bite of 1.26, which is 11° greater than the twist angles of the ferric alcaligin complex.

The stereochemical consequences of the conformational rigidity of alcaligin emerge when the $\text{Fe}_2(\text{AG})_3$ structure is compared with that of the free ligand. The former consists of three ligand fragments: two terminal ligands and one bridging ligand. The two terminal bisbidentate fragments are essentially identical: for the 20 atoms of the macrocyclic ring the rms deviation between these two fragments is as small as 0.232 \AA (Figure 8A). Figure 8c shows the conformation of the bridging ligand. While half of the molecular fragment maintains the same conformation as that of the terminal fragments, the other half deforms significantly in order to bridge two metal centers. Figure 8B shows the overlay of one terminal fragment of $\text{Fe}_2(\text{AG})_3$ with the free ligand structure;⁷ the rms deviation from the free ligand (again of the 20 ring atoms) is 0.227 \AA for the illustrated terminal fragment and 0.274 \AA for the other. This indicates that the ligand structure is not perturbed with respect to the coordination of the hydroxamate groups to the metal center. The similarity of the free ligand conformation to the terminal fragments of $\text{Fe}_2(\text{AG})_3$ is remarkable and can be viewed as resulting from an inherent structural feature of alcaligin: *the free ligand is highly preorganized for binding Fe^{3+} .*

The $\text{Fe}_2(\text{AG})_3$ structure is unique in being the first Fe_2L_3 siderophore structure crystallographically characterized and in providing the first example of the monobridged structural alternative to the triple helicates.²⁰ The latter topology has been assigned to the complexes of rhodotorulic acid and its synthetic analogues.^{18,19}

The preorganization of alcaligin not only determines the monobridged binding mode of the 2:3 ferric alcaligin complex but also readily explains the difference in affinity for Fe^{3+} between alcaligin and rhodotorulic acid. Like the two claws of a crab, the dihydroxamate siderophore alcaligin is poised for binding to a metal ion through two chelate rings. The preorganization of the alcaligin ring puts both chelate rings precisely in the correct position for the metal complex. This results in a 32-fold increase in the stability of the complex as

compared to the flexible rhodotorulic acid. However this conformational stability is a liability in the trimer complexation reaction (represented by $K_{\text{M}_2\text{L}_3}$, eq 6), with a corresponding decrease in relative stability. Overall formation of the Fe_2L_3 complex involves K_{ML} twice and $K_{\text{M}_2\text{L}_3}$ once, such that the alcaligin trimer is more stable than that of rhodotorulic acid. Alcaligin is a siderophore whose geometry is optimized for initial complexation of iron, a key to its role as a pathogen growth factor.

Summary

Two macrocyclic dihydroxamate siderophores, alcaligin and bisucaberin, have been characterized thermodynamically and structurally with respect to their $\text{Fe}(\text{III})$ coordination chemistry. Both alcaligin and bisucaberin form 1:1 ferric complexes (FeL^+) at acidic pH and 2:3 ferric complexes (Fe_2L_3) at and above neutral pH. At low ligand to metal ratios the 1:1 ferric complex of alcaligin hydrolyzes at weakly acidic pH to give a ternary complex, FeLOH . At higher pH this ternary complex dimerizes to form a novel 2:2 ferric bis- μ -oxo-bridged complex. Remarkably, the stability constants of these macrocyclic dihydroxamate siderophores differ significantly from those of linear dihydroxamate ligands. The K_{ML} of alcaligin is 32 times more stable than that of rhodotorulic acid. Unlike the achiral bisucaberin, the complexes formed by alcaligin are stereospecific. The absolute configuration of the 2:3 species is Λ . The unusual bridged structure of the Fe_2L_3 alcaligin complex provides the first example of the monobridged binding mode structural alternative to a triple helicate. It is the first siderophore found to be preorganized for metal binding.

Experimental Section

General Physical Measurements. Absorption spectra were recorded on a Hewlett-Packard 8450A vis/UV diode array spectrophotometer. CD spectra were collected on a JASCO J-500C spectropolarimeter equipped with an IF-500 II A/D converter. ^1H and ^{13}C NMR spectra were recorded at 298 K on an AM-400 spectrometer. Elemental analyses were performed by the Microanalytical Laboratory, College of Chemistry, University of California, Berkeley, CA. Analyses that were within 0.4% of the calculated values were considered acceptable. FAB mass spectra were recorded by the Mass Spectrometry Laboratory, College of Chemistry, University of California, Berkeley, CA.

Titrations. All solutions were prepared using distilled water that was further purified by passing through a Millipore Milli-Q cartridge system (resistivity = $18 \text{ M}\Omega \text{ cm}$) and then degassed by being boiled for 60 min while being purged by argon gas. Once prepared, solutions were protected from the ingress of oxygen and carbon dioxide by storing under a slight positive pressure of argon, which was purified by being passed through Ridox (Fisher) and Ascarite II (A. H. Thomas) scrubbers.

(28) Kepert, D. L. In *Inorganic Stereochemistry*; Springer-Verlag: Berlin, 1982; p 92.

A solution of 0.100 M KCl was prepared from 99.99% KCl (Fisher Scientific) and was used to maintain constant ionic strength during all titrations. Carbonate-free 0.1 M KOH was prepared from Baker Dilut-It analytic concentrate KOH and was standardized against potassium hydrogen phthalate to a phenolphthalein endpoint. Solutions of 0.1 M HCl were similarly prepared and were standardized against the 0.1 M KOH solution to a phenolphthalein endpoint. Ferric solutions (ca. 0.1 M in 0.1 M HCl) were prepared from ferric chloride hexahydrate (Aldrich, analytical grade) and standardized by EDTA titration with variamine blue B as an indicator. For all titrations, the observed pH was measured as $-\log [H^+]$. The glass electrode was calibrated in hydrogen ion concentration units by titrating 2.000 mL of standardized HCl diluted in 50.00 mL of 0.100 M KCl, with 4.200 mL of standardized KOH. The calibration titration data were analyzed by a nonlinear least squares program.²⁹

Both ligands and their ferric complexes were studied by potentiometric titration. In this study, solutions of the ligands and their ferric complexes of 0.4–1 mM were titrated at 25.0 °C. A metal to ligand ratio of 2:3:5 was used for both ligands. For alcaligin a further set of experiments were performed with a 1:1 metal to ligand ratio. The thermodynamic reversibility of each potentiometric titration was checked by cycling the titration from low to high pH and back to low pH (or the reverse). Three different titrations were conducted for alcaligin. Only one cycle of titrations was performed with bisucaberin because of the limited amount of the ligand. Potentiometric titration data were determined with the aid of an IBM 486 computer using a FORTRAN nonlinear least squares refinement program (BETA).³⁰

In the alcaligin titrations of low metal to ligand ratio (1:1) the calculated free ferric ion concentration exceeded the solubility product for amorphous Fe(OH)₃, suggesting that up to 30% of the total iron present was removed from solution. However, reducing the total iron concentration by this amount gave poor fits in the refinement of the potentiometric data while good fits were obtained by neglecting the formation of Fe(OH)₃ (goodness of fit factor = 1.8–2.8).

Spectrophotometric pH titrations were carried out to determine the metal–ligand interaction as a function of pH. The apparatus and method for spectrophotometric titrations have been described in detail elsewhere.³¹ The ferric complexes of alcaligin and bisucaberin at ca. 0.1 mM (the ratio of iron to ligand was always 2–3) were titrated in the pH range 1.8–11.0 at 25.0 °C. Three sets of data, including spectra at wavelengths between 402 and 650 nm, pH values, and respective volumes of solutions, were refined to determine the equilibrium constants for each of the complexes by using the factor analysis and nonlinear least squares refinement program, REFSPEC.^{31,32}

The formation constants of the ferric alcaligin and bisucaberin complexes were determined by competition against EDTA. For alcaligin, 25 solutions covering the pH range 6.0–8.3 were prepared containing alcaligin (ca. 0.5 mM), EDTA (ca. 5 mM), and Fe(III) (ca. 0.3 mM). The ratio of alcaligin to Fe(III) was kept greater than 3:2 for all the samples. The solutions were maintained at 25.0 °C and reached equilibrium after 2 days. Then the final pH and vis/UV spectrum (HP 8450 spectrometer; 1 cm quartz cell) of each solution were measured. It was found that the data from the solutions in the pH range 6–7.7 were useful for the stability constant determination. The pH values, absorbance spectra, and protonation constants of free ligand and EDTA were accumulated to calculate the overall formation constant. The stability constants of ferric bisucaberin were similarly determined.

Electrochemistry. Cyclic voltammograms were collected using a BAS 100A electrochemical analyzer. All potentials were measured using three-electrode circuitry with a hanging mercury drop working electrode (PAR model 303a), platinum wire auxiliary, and saturated calomel reference electrode. Voltammograms were recorded, and the

values obtained were reversible at scan rates of 100, 50, and 20 mV/s. All solutions for electrochemical examination were 1.0 M in KCl, 0.05 M each in potassium phosphate and sodium tetraborate, 1 mM in ferric chloride, and 20 mM in siderophore. The pH was adjusted using 0.1 M KOH and 0.1 M HCl.

Magnetic Susceptibility. μ_{eff} was determined in 10:1 D₂O/dioxane solution at pH 2, 7, and 11 using the Evans method.³³ At each of three pHs (2.5, 7.4, 11.5), three different solutions of 0.06 M siderophore complex with 2:3.5 Fe:AG stoichiometry were tested and differences in dioxane peaks were measured. Deuterium concentration was adjusted with 0.1 M DCl or 0.1 M NaOD, both in D₂O.

Synthesis of the Ferric Alcaligin Complex (Fe₂(AG)₃). A 74.36 mg sample of alcaligin·2H₂O was dissolved in 20 mL of H₂O/CH₃OH (1:1 v/v). To this was added an excess of freshly precipitated and carefully washed (by centrifuge) Fe(OH)₃. The mixture was stirred at room temperature for 24 h, during which time most of the ferric hydroxide dissolved and the solution turned a dark orange-red. The unreacted Fe(OH)₃ was removed by filtration. After removal of the solvent, a dark-red solid was obtained, which was passed through a lipophilic Sephadex LH-20 column (15 × 2 cm) eluted with MeOH. A single red-orange band was observed, collected, and then dried to give 67.2 mg of a red product. Vis/UV, aqueous solution (pH = 7.0): λ_{max} 428 nm, ϵ 2400 cm⁻¹ M⁻¹/Fe. Analyzed by +FAB-MS: *m/e* 1319.2 (Fe₂(AG)₃H)⁺.

Structural Solution. A deep red needle crystal of Fe₂(AG)₃·25H₂O (0.50 × 0.17 × 0.05 mm) grown from a solution of H₂O/CH₃CN was mounted on a quartz fiber in paratone oil. All measurements were made on a Siemens SMART³⁴ diffractometer at -148 °C with graphite-monochromated Mo K α radiation.³⁵ Cell constants and an orientation matrix obtained from a least squares refinement using the positions of 8192 reflections in the range 2.1 < 2 θ < 46.5° corresponded to a primitive orthorhombic cell with dimensions *a* = 13.3374(4) Å, *b* = 16.1879(5) Å, *c* = 37.886(1) Å, *V* = 8179.7(4) Å³. Systematic absences uniquely determined the space group as P2₁2₁2₁ (No. 19); for *Z* = 4 and *fw* = 1769.3, ρ_{calc} = 1.44 g/cm³. An arbitrary hemisphere of data was collected using an ω scan technique with an image width of 0.3° and total image collection time of 30 s. The intensity data were extracted with the program SAINT³⁵ using an integration box with 1.0 (XY)° × 0.5 (Z)° parameters and a maximum 2 θ of 46.5°. Of the 339 16 reflections integrated, 6521 were unique; equivalent reflections were merged, and no decay correction was needed. A linear absorption correction was made using the program XPREP (*T*_{max} = 0.969, *T*_{min} = 0.880). The structure was solved by direct methods (SAPI90).³⁶ After full-matrix least squares refinement³⁷ on *F*, based on 5512 (*I* > 3.0 σ (*I*)) reflections and 995 variable parameters, *R* = 0.053, *R*_w = 0.068. All non-hydrogen atoms of the complex were refined anisotropically. The assignment of the structure's absolute configuration conforms to that of the free ligand alcaligin²² and was determined by the Bijvoet technique; inversion of the structure and refinement caused a significant increase in *R* value. All calculations were performed using the teXsan³⁸ crystallographic software package of Molecular Structure Corporation.

Equilibrium Calculations. Species distribution curves were calculated with the program SOLGASWATER³⁹ using the protonation and stability constants determined in this work and Fe(III) hydrolysis constants from ref 40. These hydrolysis constants were also included as fixed parameters in all of the solution equilibrium measurements.

(29) Martell, A. E.; Motekaitis, R. M. *Determination and Use of Stability Constants*; VCH: New York, 1988.

(30) Franczyk, T. S. Ph.D. Dissertation, University of California at Berkeley, 1991.

(31) Scarrow, R. C. Ph.D. Dissertation, University of California at Berkeley, 1985.

(32) Turowski, P. N.; Rodgers, S. J.; Scarrow, R. C.; Raymond, K. N. *Inorg. Chem.* **1988**, *27*, 474–481.

(33) Evans, A.; Hancock, R. D.; Martell, A. E.; Motekaitis, R. J. *Inorg. Chem.* **1989**, *28*, 2189.

(34) SMART; Area-Detector Software Package; Siemens Industrial Automation, Inc.: Madison, WI, 1995.

(35) SAINT; SAX Area-Detector Integration Program, V4.024; Siemens Industrial Automation, Inc.: Madison, WI, 1995.

(36) SHELXS-86; Institut für Anorganische Chemie der Universität: Göttingen, FRG, 1986.

(37) DIRDIF92; the DIRDIF program system. Technical Report of the Crystallography Laboratory, University of Nijmegen: Nijmegen, The Netherlands, 1992.

(38) teXsan; Crystal Structural Analysis package; Molecular Structural Corporation, 1985 and 1992.

(39) Eriksson, G. *Anal. Chim. Acta* **1979**, *112*, 375–383.

(40) Baes, C. F.; Mesmer, R. E. *The Hydrolysis of Cations*; Wiley: New York, 1976.

Acknowledgment. This research was supported by the National Institutes of Health through Grant AI 11744 and by a University of California Systemwide Biotechnology Grant. We thank Professor Y. Okami for the generous gift of the siderophore bisucaberin and Dr. Christopher J. Sunderland for experimental assistance.

Supporting Information Available: An illustration of the metrical parameters of the two iron chelate centers in the $\text{Fe}_2(\text{AG})_3$ structure and tables of bond distances, angles, positional coordinates, and thermal

parameters (13 pages). Ordering information is given on any current masthead page. Crystal structure data for the structure, including atom coordinates, were deposited with the preliminary communication of the structure.²¹ Further details of the crystal structure investigation are available on request from the Director of Cambridge Crystallographic Data Center, 12 Union Road, GB-Cambridge CB21EZ, U.K., on quoting the full journal citation.

IC9810182